

Models for reticle performance and comparison of direct measurement

Terrence E. Zavecz^{*}, TEA Systems
Ray Hoobler, Nanometrics
Mircea Dusa, AMSL

ABSTRACT

It's commonly reported that a difference exists between directly measured reticle feature dimensions and those produced in the final lithographic image. Quantifying this mask error function (MEF) and the sources of the perturbation has been the topic of many papers of the past several years. Past studies have been content to evaluate these functions by statistical averaging thereby neglecting the potential influence of process and exposure contributions.

The material presented here represents the findings of an extensive study of reticle-process interactions. Phase I of the evaluation consisted of focus and dose exposures of the reticle and subsequent modeling of the full-profile response. This analysis provided extensive information on the optimum-printed feature profiles while removing the contribution of across-field focus variations.

The reticle was directly characterized using both conventional SEM and a new Nanometrics OCD Scatterometer technique. The full-field modeled response surface of the directly measured feature characteristics are then used to calculate the across-field MEF and provide an improved estimate of the true response of the feature to exposure.

Phase II of the analysis turns its attention to characterization of the full-wafer process response. Both the modeled and directly measured reticle surfaces were removed from Scatterometry measured full-wafer exposures. Normal process variations consisting of photoresist and ARC thickness volatility are next used to show the response of the printed feature. Finally a summary of the relative contribution of each process perturbation to the feature profile error budget is discussed.

Keywords: Lens, aberration, perturbation, process control, SEM, Scatterometry, scanner, semiconductor, model, wafer

1. INTRODUCTION

The Mask Error Factor (MEF) was shown by Conley et al. to be a feature-size bias that responds nonlinearly to imaging setup of the process and exposure tool as well as feature characteristics such as the duty cycle.[1] The study demonstrated the fact that MEF values respond to many influences including the ever-changing incidental focus of the exposure and film-stack uniformity.

The volatility of MEF calculations is further demonstrated by a paper by Harris et al that calculated the differing values for vertical and horizontal lines under various exposure conditions.[2] These experiments illustrated the fact that features respond very differently when subjected to varying aspects of off-axis illumination.

Characterizing the full- field exposure MEF variation is critical when attempting to link simulation model response to empirical data performance or when attempting to extract the true feature profile response to perturbations introduced by process variants such as imaging aberrations and film thickness nonuniformity. A formalization that accounts for film as well as profile and process variants is needed to properly characterize the transitional characteristics of the object-to-image transfer process of empirical data.

A formalization for IntraWafer Critical Dimension Uniformity (CDU) characterization by Dusa et al. presented a general feature perturbation model as:

$$FR_a = \Delta_a * D_m < 1$$

^{*} Contact: tzavecz@TEAsystems.com phone: (+01) 610 682 4146, <http://www.TEAsystems.com>

Where FR_a is the feature response of feature a to a process disturbance Dm and Δ_a is the sensitivity coefficient.[3] Figure 1 summarizes the process disturbances considered by the authors.

Equation <1 can be used to characterize any measured feature in the lithographic process by expanding the process disturbance terms into perturbation specific source components in a format similar to:

$$FR_a(x, y) = IF_p(x, y) + W_p(x, y) + DD(x, y) + r \quad <2$$

Where the terms of equation <2 now describe the response of a feature located at position (x, y) as:

- ⌘- $IF_p(x, y)$: IntraField periodic signature
 - ⌘ Reticule component and a systematic –within-wafer, periodic component
 - ⌘ Describing the scanner field (slit and scan signatures)
- ⌘- $W_p(x, y)$: feature response variability
 - ⌘ This component is primarily a result of the “whole-wafer-at-a-time” process steps, characteristic to resist and track.
- ⌘- $DD(x, y)$: Die-to-Die variability
 - ⌘ variations in discrete scanning disturbances such as effective dose, the incidental focus or scan direction.
- ⌘- r : the residual component

The conclusions of the application of equation <2 recognized that the largest CDU error components, of those shown in figure 1, were contributed by the post-exposure bake and bottom anti-reflective coating thickness nonuniformity. In fact, the exposure tool contributed components of IF_p amounted to only about 20% of the error budget. Yet, within this 20% lies the volatility of the MEF. An expanded treatment of the IntraField periodic signature must be addressed to implement a good linkage between simulation and empirical data metrology.

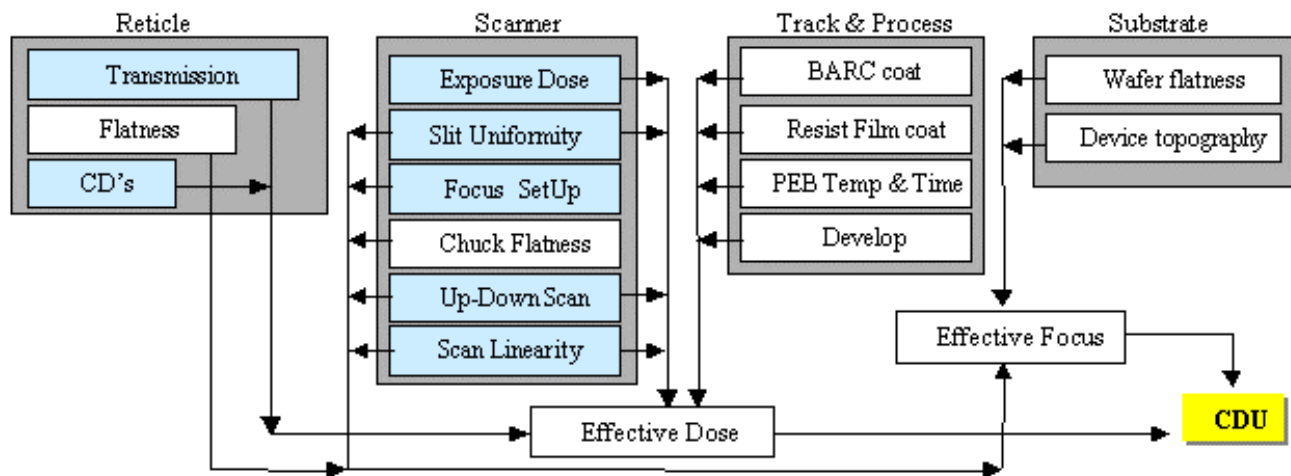


Figure 1: Sources of CD non-uniformity
 Perturbations of the nominal dose and focus accounted for in equation <2. IntraField perturbations addressed are shown as highlighted.

2. MASK ERROR FACTOR MODELED

The MEF is simply defined as:

$$MEF = \frac{CD_{Photoresist}}{(CD_{Mask} * Reduction)} \quad <3$$

Where we can then address the definition in the formalism of equation <2 as:

$$IF_{p(x,y)} = IF_{Reticle} + MEF \quad <4$$

or

$$IF_{p(x,y)} = IF_{Reticle} + IF_{Slit, scan aberrations} + IF_{Effective Dose, Focus} + IF_{Resist} + IF_{flare} + IF_{scatter} \quad <5$$

The $IF_{Reticle}$ component will be the greatest contributor to the IntraField perturbations. The $IF_{Slit, Scan}$ contributions can be directly modeled from the data and will be addressed later in the dissertation. What remains is to address the analysis to a method of determining or eliminating the perturbations introduced by the effective focus & dose, photoresist, flare and scatter.

Consider now the common application of the process window analysis commonly embodied by equation 6: [4]

$$FR(x, y) = \sum_{m=0}^M \sum_{n=0}^N \alpha_{nm} \left(1 - \frac{E_s}{E} \right)^n F^m \quad <6$$

Where we now describe the feature response as that for a measured entity located at position (x,y) on the exposure field. The variables involved in this equation use the common definitions of E as the exposure dose, E_s being the nominal dose to achieve image size and F being the defocus of the exposure.

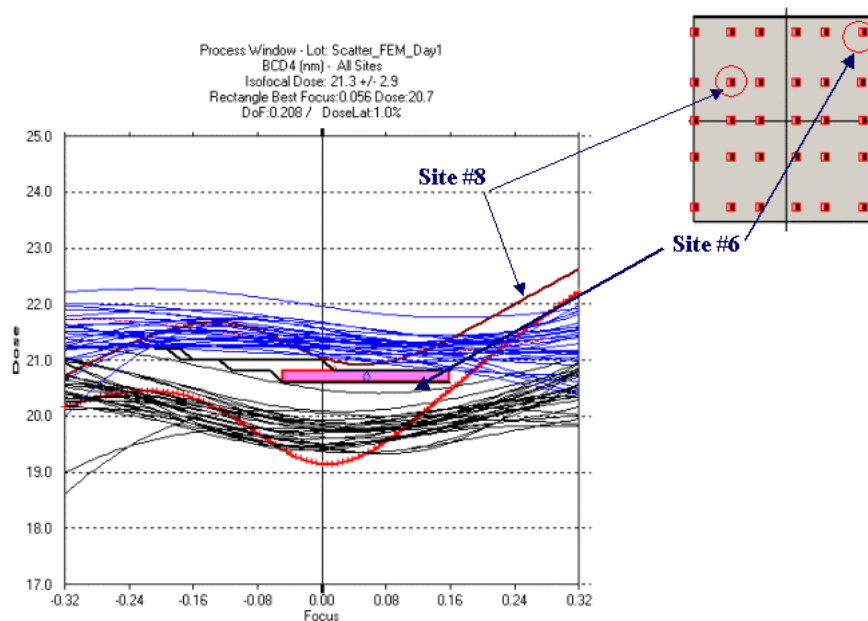


Figure 2: Process window for the full exposure field of 80 nm features

The composite process window for 30 measured sites on a field is limited by the curve for Site #8 and the aberrated response of site #6.

The reason for defining equation 6 as a particular point on the exposure field becomes clear if the process window graph of figure 2 is examined. The response of site #8 is a metrology error that is easily corrected with proper data culling. The overall spread of the boundary curves in the plot reflects the variation across the exposure field due to reticle and exposure perturbations. Observe the behavior of site #6 as an extreme example that results from lens and scan aberrations. The response of site #6 is real and will restrict the size of the operational window and strongly contributes to the variability of the process MEF.

Equation 5 shows that one component of the MEF involves the contribution of the effective dose and focus of the measured feature in the field. Minimizing this term requires that we determine and remove the influence of variable focus and dose across the exposure. These factors can be removed through an extension of a commonly performed analysis for the industry, the focus-exposure matrix (FEM) analysis of the process window. The method used for this analysis is shown in the next section and explained in detail in a separate paper by Zavec.[5]

3. PHASE I – MODELED CORRELATION OF WAFER AND DIRECT-RETICLE METROLOGY

3.1 Removing the influence of process and effective focus and dose

Characterization of the effective-focus and dose MEF contributed by the process and exposure tool employed a typical 193 nanometer (nm) lithography process for 100 nm --final size—Moly features. An ASML AT1100 scanner with 0.75 NA annular illumination exposed an 11x11 matrix of 1:1 gratings with full field coverage.

The wafers were measured using a Nanometrics NanoOCD 9030 tool with normally incident rotating polarized light. This experiment modeled Bottom Critical Dimensions (BCD), Resist Thickness (Tr), the Side-Wall-Angle (SWA), bottom anti-reflective coating (BARC) thickness and reported the mean square error (MSE) of each modeled site response.

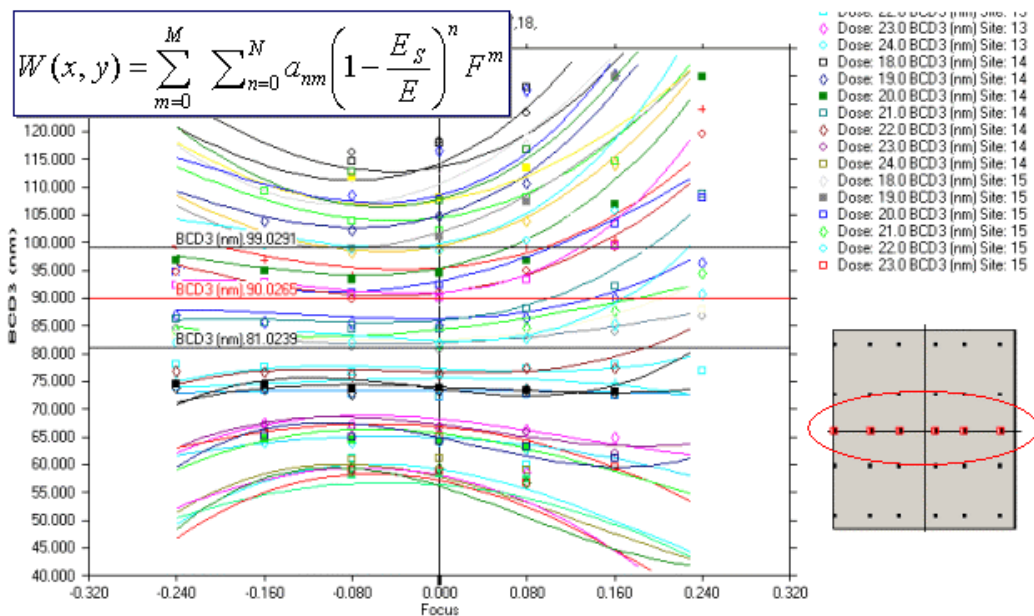


Figure 3: Bottom CD focus response across center slit

Weir PW software from TEA Systems is used in the analysis to derive the extended process window, provide surface models for wafer, field, slit and scan and estimation of the photomask (mask) contributed MEF.

The wafer exposure involved a full-field focus-exposure matrix (FEM) that extended only a limited range through focus and dose. The results shown in figure 3 for sites located across the slit location for the center of the exposure field illustrate the variability of optimum focus and dose across a single slit.

Applying the process surface of equation <6 to the entire field yields the family of curves shown, partially, in figure 3.

The first order derivative of equation <6, evaluated for each exposure-dose, yields the optimum focus for each site, the feature size at this “Best Focus” location and the optimum Depth of Focus (DoF) for the site’s dose. Then by reassembling the calculated optimum BCD value obtained for each of the 121 sites across the exposure field, the

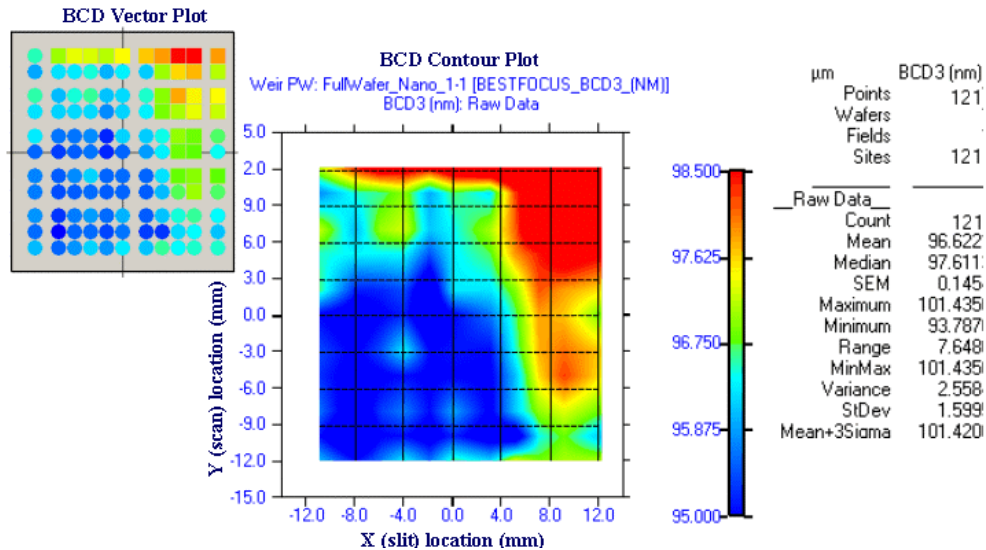


Figure 4: Bottom CD response at 121 measured sites under optimum focus and dose

optimal BCD uniformity plot of figure 4 is derived.[5]

The BCD distribution derived by this method uniquely describes the process’s ability to replicate the features on the mask since the perturbations contributed by IntraField focus variables are fully removed, the across-process dose variation are minimized and the individual site metrology random error is removed through the surface fitting procedure. This surface embodies the optimized image response with the “ $IF_{(Effective\ Dose\ \&\ Focus)} + IF_{Resist} + IF_{flare} + IF_{scatter}$ ” components of MEF in equation <5 removed. The BCD values shown however still contain contributions from the $(IF_{Reticle} + IF_{Slit, scan\ aberrations})$ IntraField components.

3.2 Direct Reticle Metrology

The test reticle used consisted of 100 nm final size, 1:1 duty cycle features in an 11x11 matrix of MiSiON on quartz. A chuck modified Nanometrics NanoOCD 9010M mask tool was used to directly measure the reticle features with an OCD model optimized for the reticle-substrate and films.

Since the application of an OCD tool to direct reticle feature measurement is novel, the mask was also measured with an Hitachi CD-SEM for reference.

The Hitachi data statistics were found to contain a mean value of 418.3 nm with maximum/ minimum excursions of 433.7 nm and 405.0 nm respectively. A statistical comparison of the Hitachi measurements and the optimized BCD surface of figure 4 was used to determine a single MEF+ value for the system where MEF+ is defined as:

$$MEF+ = Demagnification + MEF \quad >7$$

The proper MEF+ value is determined by the following procedure:

For each Dose:

BCD on Wafer			
	Reticle	CD_final Delta (nm)	Dose
MAG & MEEF=	4.3282		15.0
Ret Max	439.9194	101.6400	-1.4369
Ret Min	393.7244	90.9670	2.6051
<hr/>			
MAG & MEEF=	4.3910		15.5
Ret Max	448.6857	102.1830	-3.4128
Ret Min	-198.2406	-45.1470	137.3811
<hr/>			
MAG & MEEF=	4.3236		16.0
Ret Max	444.1506	102.7280	-2.4171
Ret Min	400.5864	92.6520	1.0208
<hr/>			
MAG & MEEF=	4.3292		16.5
Ret Max	439.1410	101.4360	-1.2568
Ret Min	406.0266	93.7870	-0.2371
<hr/>			
MAG & MEEF=	4.3645		17.0
Ret Max	449.9643	103.0970	-3.7265
Ret Min	-370.1860	-84.8180	177.6127
<hr/>			
MAG & MEEF=	4.3293		17.5
Ret Max	438.7891	101.3480	-1.1709
Ret Min	407.7191	94.1760	-0.6281
<hr/>			
MAG & MEEF=	4.3186		18.0
Ret Max	449.2860	104.0350	-3.6090
Ret Min	398.3437	92.2390	1.5413

Table 1: Optimum MEF+ calculation

- ⚡ Calculate MEF+ for each dose
 - ⚡ $MEF+ = \text{Reticle mean size} / \text{BCD size @ Best Focus}$
- ⚡ Calculate BCD Point-Spread if it were on reticle
 - ⚡ $\text{Reticle} = (\text{BCDwafer} * \text{MEF+})$
- ⚡ Determine Delta
 - ⚡ Difference between (BCD on wafer) - (Reticle on wafer)
 - ⚡ $\text{Delta} = (\text{Reticle} / \text{MEF+}) - \text{BCD}$
 - ⚡ For max, min values at each dose

The optimum MEF+ value is defined as the value at which the lowest Delta values for are obtained and has been bordered in red on Table 1. *Note that the dose values shown here are arbitrary and should not be considered as absolute representations of the process used. This will have no influence on the final results.*

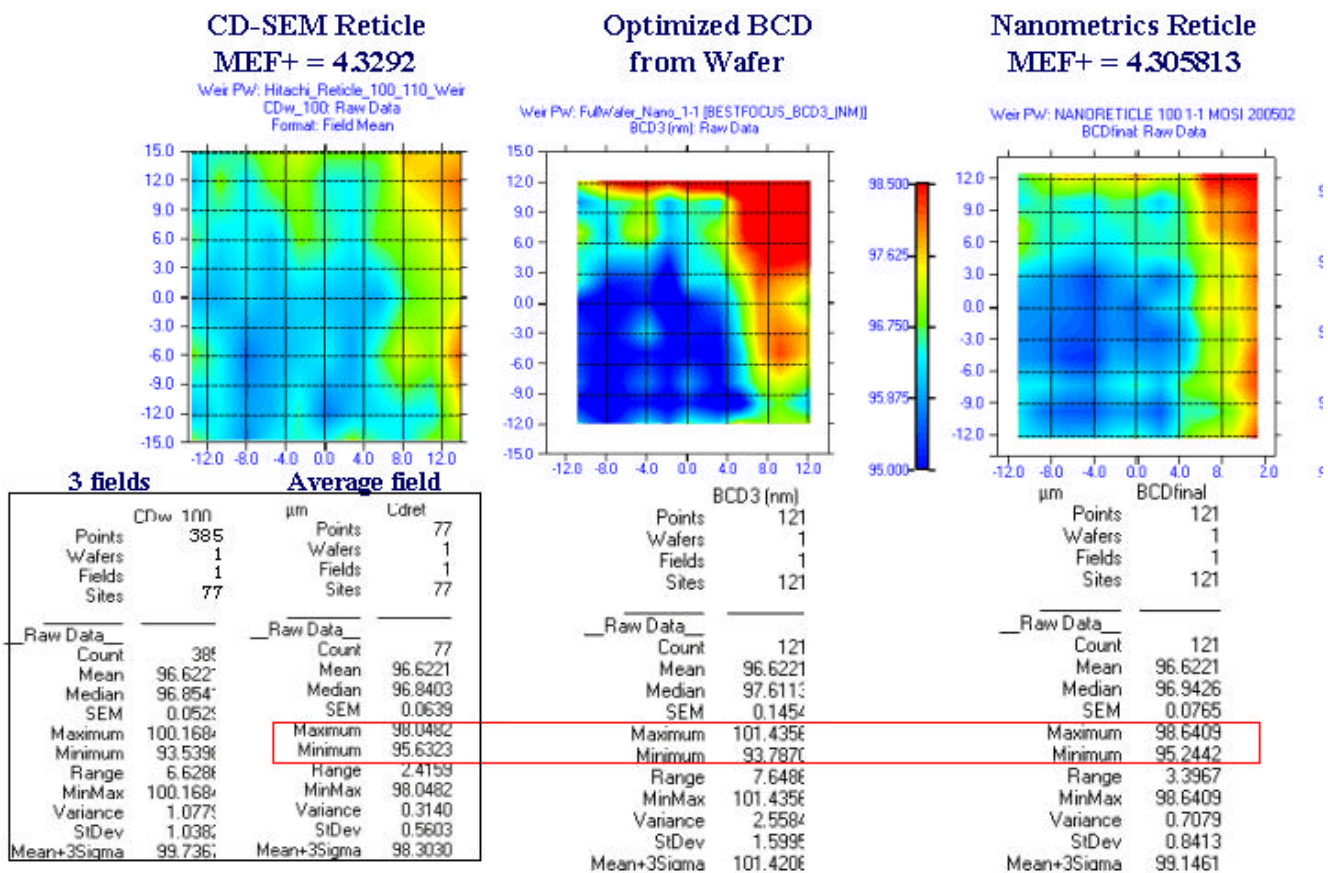


Figure 5: Optimized BCD comparison with CD-SEM and OCD reticle metrology

The MEF+ values are then used to convert the reticle measured metrology to wafer-final values for comparison with the Optimized BCD surface. The OCD metrology was handled in a like manner and the results are compared in figure 5.

The CD-SEM data covered a larger area than the BCD and OCD measured data and also represented three sequential measurements of 77 data sites. OCD metrology measured 121 sites one time across the reticle.

Examination of the maximum/ minimum values bracketed with the red box in figure 5 shows less than 1 nm range difference between the CD-SEM and OCD metrology for the reticle validating the OCD reticle measurement method.

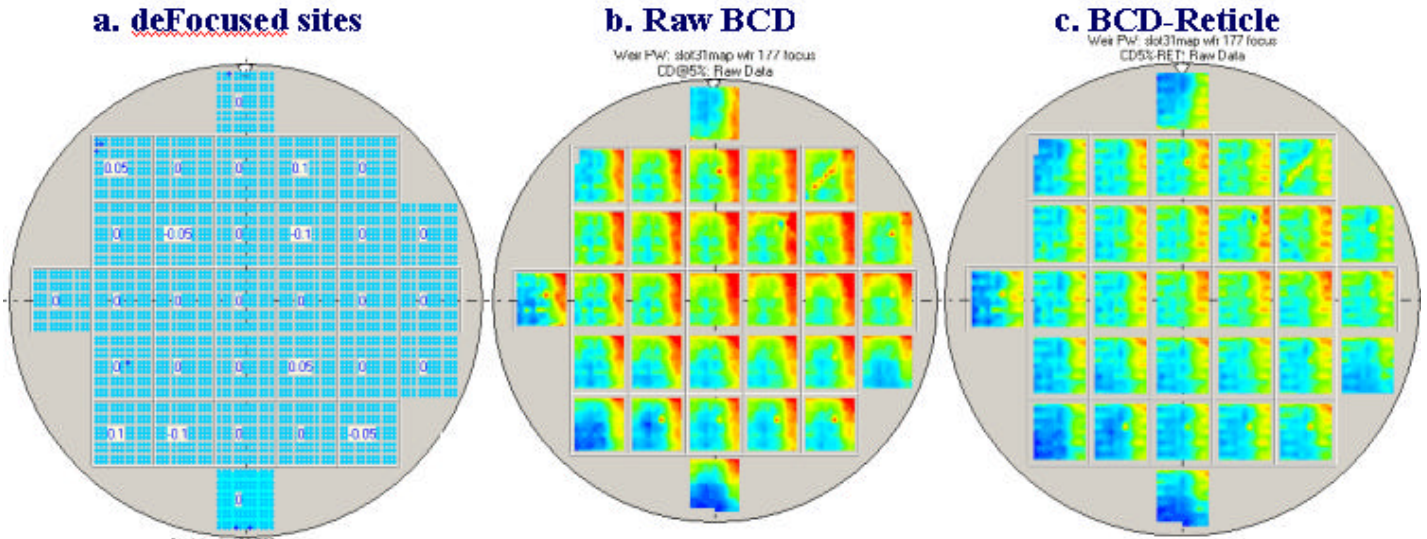


Figure 6: Full wafer exposure with a) 1% & 2% focus offsets, b) as-measured BCD values and c) the BCD-RET (Reticle)
 The reticle thus contributes a range of 3.4 nm to the BCD error budget.

The Optimized BCD pattern contains a signature very much like the OCD pattern. The method is an excellent means of validation for reticle feature quality and can be used as an estimation of optimal feature size distribution for any process. The Optimized BCD plot shown in the center of figure 5 exhibits a slight increase in BCD range of 4.3 nm over that of the SEM and OCD measured data. This increase represents the slit and scans contributions to the MEF as will be shown in the next section.

4. PHASE II: SLIT, SCAN AND PROCESS CONTRIBUTIONS

4.1 Full wafer response

A wafer was exposed at optimum focus with six sites offset in focus by 1% of the DoF (+/-0.05um) and 2%, see figure 6a. Figure 6b, measured by the OCD system, shows a strong correlation to the reticle signature of figure 5. Several of the fields contain some points that represent exposures that were damaged during processing; see the field exposure in the upper right corner of figure 6b.

The Reticle values measured by the CD-SEM were interpolated and subtracted from the BCD data to generate the BCD-RET contour plot of figure 6c. The BCD-RET variable now represents the process response of the features without the reticle contribution and will be used to determine the true process and exposure response. Notice that within this contour

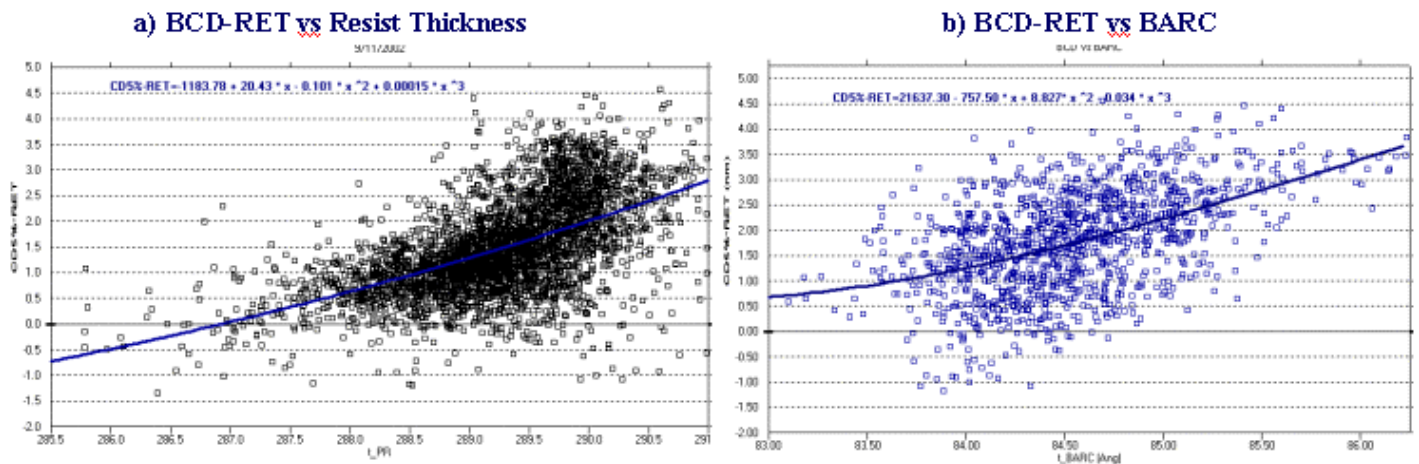


Figure 7: Process response of BCD-RET variable to a) Resist Thickness and b) BARC

the slight variations perturbed by the focus offset fields cannot be easily seen. These offsets will be addressed in section 4.3.

4.2 Process Response

The perturbations of the focus offsets provide some spread in the absorption characteristics of the photoresist resulting in slight changes in thickness. Similarly, the BARC thick will vary slightly across the wafer and the BCD-RET variation is plotted against each variable in figure 7. In both cases, the anticipated sinusoidal response of the BCD-RET feature can be observed.

A significant spread in the response still exists and can be attributed to the perturbations of the slit and scan. Extraction of the contributions of the exposure requires some additional modeling.

4.3 Exposure characteristics of the slit and scan

A scanner image in photoresist is generated by two independent systems, the slit and the reticle-scan stage. The feature perturbation response can therefore be characterized by: [5]

$$IF_p(x,y) = IF_{slit}(x) + IF_{scan}(y) + r \tag{8}$$

$$IF_p(x,y) = \sum_{Rows} \sum_{n=0}^4 a_n x^n + \sum_{Columns} \sum_{j=0}^4 a_j y^j + r \tag{9}$$

Where r represents the random residual contributions. The individual contributions of slit and scan are adequately described by a simple 4th order polynomial because of the one-dimensional nature of the analysis. The coefficients in turn describe the physical response of the slit and scan at the X-column and Y-row locations on the field with the a₀ term representing the offset, a₁ the tilt etc.

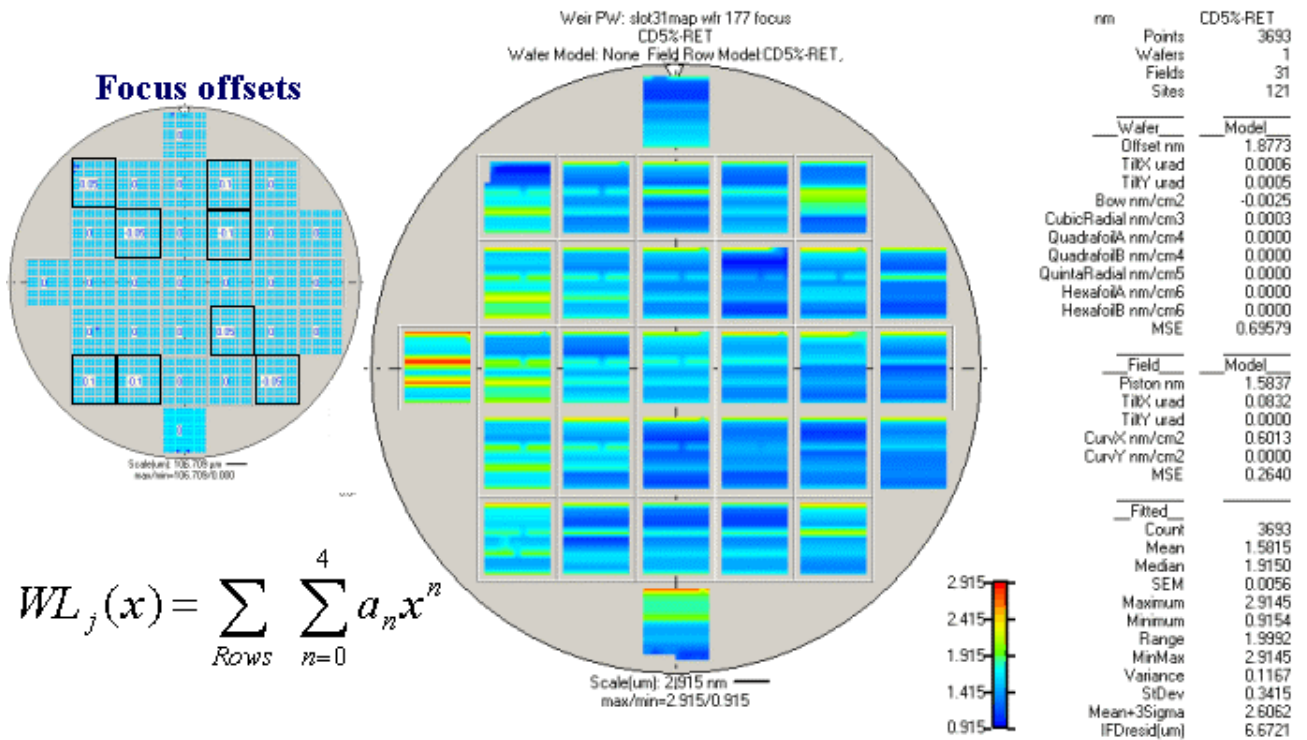


Figure 8: Scan-slit lens perturbations of BCD-RET, a₀ offset coefficient contour plotted

Lens-Slit Response

The BCD-RET field modeled by equation <9 allows a direct plotting of the BCD-RET perturbations contributed by the lens in figure 8. In this case, the slit response is modeled on each row of each field and the center contour plot of the figure displays only the contributions of a_0 to illustrate relative offsets of each field. The six dice that were offset in focus by 1% and 2% are shown in the wafer graphic on the upper left of the figure. An examination of the central contour plot now shows the response of the process to these small focus perturbations.

Figure 9 reproduces the lens perturbation response of BCD across the slit. This lens replicates an aberration-free image in the left side of the field that is amplified on the right-side of the exposure. The box plot graph on the left side of figure 8 illustrates this signature for both the lens contributed and scan-contributed components of the exposure. The

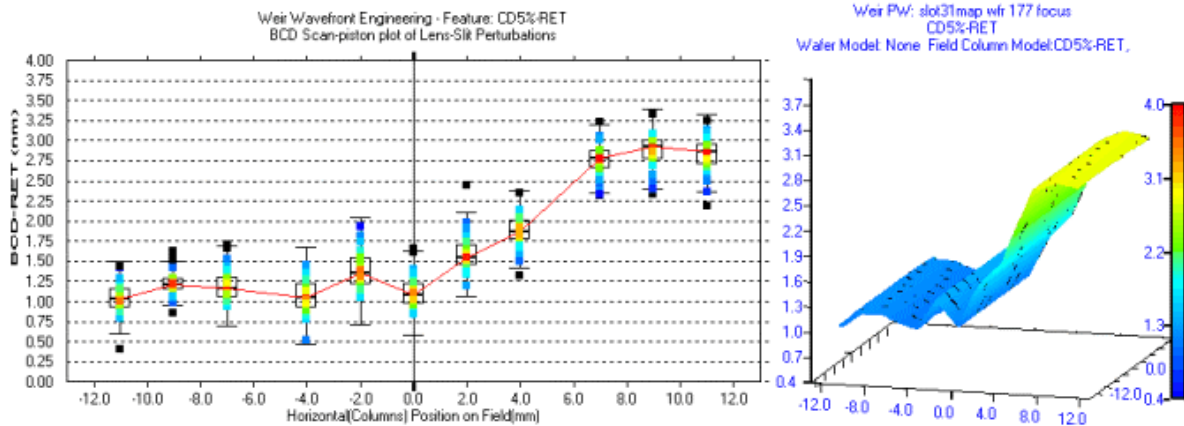


Figure 9: Lens-slit BCD aberration profile as a BoxPlot (left) and using the a_0 coefficient of the model (right)

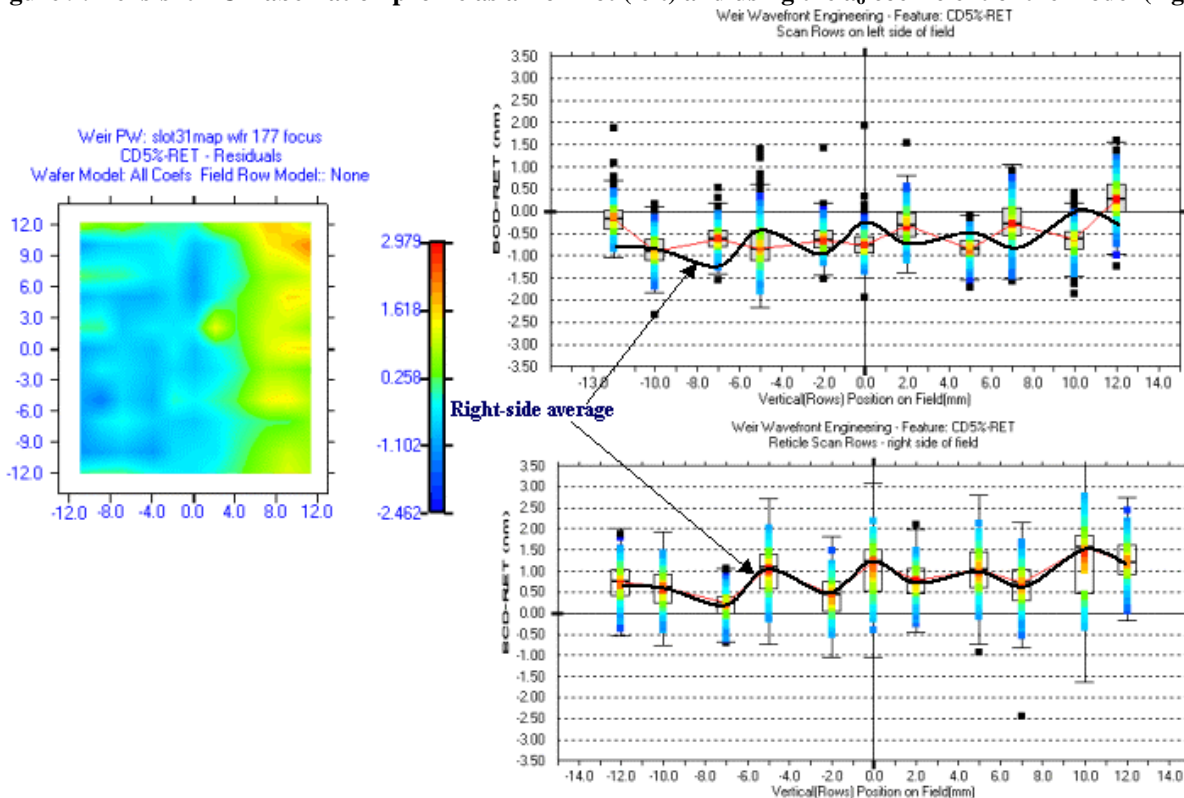


Figure 10: Left: Modeled BCD-RET response field
Upper Right/ Top: Boxplot of each row response for the left side of the field
Upper Right/ Bottom: Boxplot of each row response for right side of the field

population spread on each box plot, from the scan, is color-coded with the population median at each point in the field plotted in red and connected by the red-median line. Populations then expand with the 4th quartile of the box corresponding to a deep blue color and outlier points are plotted in black.

The a_0 coefficient of the model, again illustrating the lens contribution, is plotted on graph located on the right side of figure 9. Lens perturbations contribute 2 nm to the BCD error budget.

Reticle-Scan Response

The reticle-stage-scan response is more complex than that of the lens-slit as shown in figure 10. The scan response on the left-side of the field is plotted in the boxplot located on the lower right of figure 10. Here the median of each row's population is outlined in the dark-black curve connecting the medians of each row's population boxplot.

The upper boxplot of figure 10 shows the response of the left side of the exposure field. Superimposed on this graph is the black-median line from the right side average plotted below and described in the paragraph above. Note the relative response of the two population medians. The left side of the field's BCD variation is 180° out of phase with features on the right side resulting in a left-to-right perturbation shift of 0.5 to 0.75 nm.

This phased-tilt behavior is adequately modeled in the a_1 coefficient of equation <9 and plotted in figure 11. We can see from the figure that the reticle-scan stage wobble is contributing 1.25 nm to the BCD error budget. Overall Tilt of the stage contributes 3 nm to MEF variations in BCD.

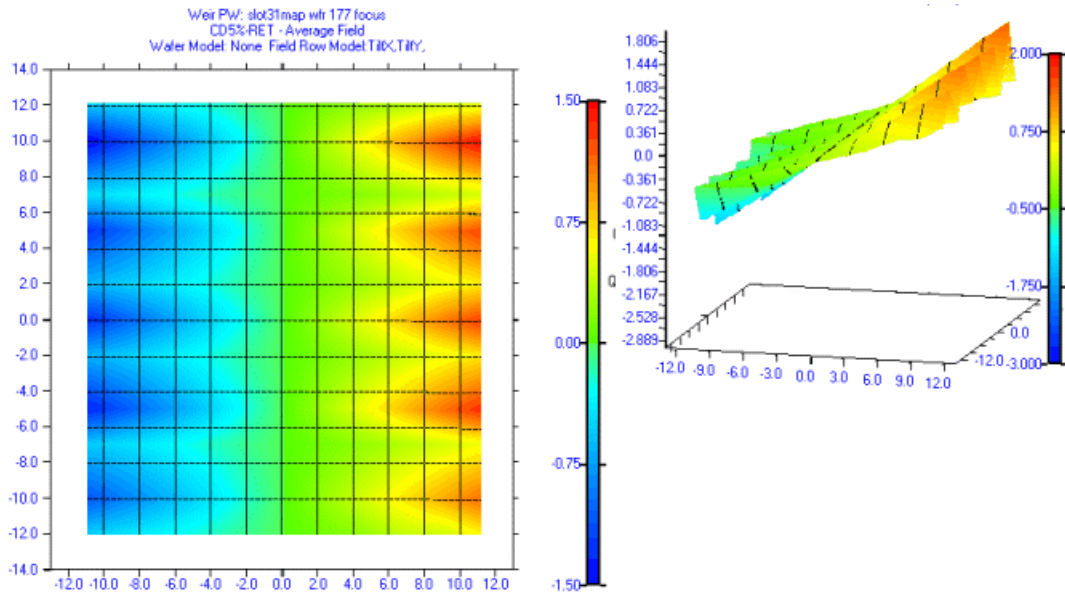


Figure 11: BCD-RET perturbations contributed by slit-tilt coefficient a_1 across the exposure

5. CONCLUSIONS

We have developed a model that can take much of the variability out of the mask error function associated with image transfer into the photoresist. The model is capable of taking optical-scatter measured profile data and correlating the various feature responses directly to their corresponding mask structures.

Photomask data can be directly measured by SEM and, with recent developments by the vendor, by using optical scatter models. Averaged SEM and optical scatter measurements (OCD) correlate to better than 1 nm (final size). Wafer measured OCD data of Bottom Feature Profiles taken in a focus/dose matrix can also be correlated to the directly measured photomask. The full-field perturbation signatures for both mask and wafer correspond highly with the wafer population slightly expanded by 3.4 nm. This expansion represents the contributions of process and exposure artifacts to the BCD exposure budget.

Removing the fixed reticle feature perturbations from fixed-focus wafer exposures provides that ability to finely analyze both process and exposure artifacts in the image transferal process. Feature size response to thickness changes in photoresist and BARC reflect the anticipated sinusoidal response.

Analysis of the lens-slit and reticle-scan perturbations provides a method of detecting feature response to focus changes as small as 1% of the focus budget (0.05 μm defocus). Finally a model has been presented that provides a method of determining the perturbations introduced on the features by lens aberrations across the slit and during the scan of the reticle-stage. These perturbations, in the system used for the analysis, displayed a 3nm perturbation of the Bottom Critical Dimensions of 3 nm due to slit tilt and 1.25 nm from wobble (pitch) of the stage during scan.

The lens-slit perturbations amounted to less than 2 nm of aberration occurring primarily across the right side of the exposure field.

REFERENCES

1. W. Conley, C. Garza, M. Dusa, R. Socha, J. Bendik, c. Mack, "The MEEF shall inherit the earth", SPIE (2001), vol 4346-27
2. P.Harris, M. McCallum, "Compensation for imaging errors in EUV Lithography", SPIE (2004) vol. 5374 – 98, pp. 833 to 838
3. Mircea Dusa, Richard Moerman, Bhanwar Singh, Paul Friedberg, Ray Hoobler, Terrence Zavecz, "Intra-wafer CDU characterization to determine process and focus contributions based on Scatterometry Metrology", Proc. SPIE (2004), Vol. 5378-11
4. C. Ausschnitt, S. Cheng, "Modeling for Profile-Based Process-Window Metrology", SPIE (2004) vol. 5378, pp 38 – 47
5. T. Zavecz, "Full-field feature profile models in process control", Proc. of SPIE (2005) Vol. 5755-16